Preparation and Characterization of Ni–TiO₂ Nanocomposite Coatings Produced by Electrodeposition Technique

Isil Birlik[1]*, N. Funda Ak Azem[1], Mustafa Toparli[1,2], Erdal Celik[1,2], Tulay Koc Delice[3], Sidika Yildirim[3], Onur Bardakcioglu[3] and Tuncay Dikici[4]

[1] Department of Metallurgical and Materials Engineering, Dokuz Eylul University, Izmir, Turkey, [2] Center for Fabrication and Applications of Electronic Materials (EMUM), Dokuz Eylul University, Izmir, Turkey, [3] The Graduate School of Natural and Applied Sciences, Dokuz Eylul University, Izmir, Turkey, [4] Department of Materials Science and Engineering, Izmir Katip Celebi University, Izmir, Turkey

In this paper, Ni–TiO₂ nanocomposite coatings with different sizes of TiO₂ nanoparticles were successfully prepared by electrodeposition process from a nickel electrolyte in which the TiO₂ nanoparticles were suspended. The influence of relevant deposition parameters on the nanocomposite coating characteristics was discussed. X-ray diffractometer has been applied in order to investigate the phase structure of the nanocomposite coatings. The surface morphology of nanocomposite coatings was characterized by a scanning electron microscopy equipped with an energy dispersive spectroscopy. The electrodeposited nanocomposite coatings obtained at different deposition parameters were evaluated for their mechanical and corrosive properties. Obtained results show that the size of TiO₂ nanoparticles and applied current density during deposition process has a direct effect on mechanical and corrosive properties of nanocomposite coatings. Increasing current density and smaller nanoparticle size has affirmative effect on mechanical properties, whereas corrosion resistance of nanocomposite coatings deposited at 3 A dm^{-2} current density are higher than the coatings prepared at higher current density values.

Keywords: electrodeposition, coating, Ni–TiO₂ nanocomposite, corrosion, mechanical properties

INTRODUCTION

Ni-based coatings have been widely used in several applications in form of single phase (Ni and Ni alloys) and Ni matrix composites/nanocomposites because of their good mechanical properties, high corrosion, and wear resistance (Miguel et al., 2015). Several techniques, such as thermal and plasma spraying, chemical vapor deposition, physical vapor deposition, sol–gel, and electrodeposition, have been investigated for developing composite coatings. Electrochemical deposition from aqueous electrolyte solutions gained importance as an attractive and versatile surface finishing technique. This technique has been considered as one of the outstanding techniques for producing composites due to remarkable advantages, such as simplicity, low cost, high deposition rate, uniformity of thickness, high purity, low porosity, no shape limitations, ease control of microstructure, and chemical composition of the deposits (Benea et al., 2014; Goldasteh and Rastegari, 2014; Walsh and Leon, 2014; Beltowska-Lehman et al., 2016), and can be conducted at normal pressure and ambient temperature with low cost, high deposition rates, and homogenous particle distribution (Gül et al., 2012).

Electrodeposition of composite coatings for the production of metal matrix composites is composed of a metal matrix electrolyte and dispersed second phase particles (Yang et al., 2009). Incorporating a great variety of particles, such as hard oxides and carbides (SiO$_2$, Al$_2$O$_3$, TiO$_2$, CeO$_2$, *SiC*, and WC), solid lubricates (PTFE, Graphite, and MoS$_2$), multiwall carbon nanotubes, graphene, and diamond, into the metal matrix have been used to enhance the lifetime, performance, corrosion resistance, wear resistance, and hardness of the metal matrix composite coatings (Katamipour et al., 2014; Lia et al., 2016; Thurber et al., 2016).

Among these reinforcements, TiO$_2$ is one of the most important oxides used in the engineering materials, due to its applications in various processes, such as photo-induced hydrophilic coatings and self-cleaning devices, waste water treatment, degradation of pesticides, production of hydrogen fuel, pigments, dye-sensitized solar cells, and, more recently, monitoring of air contaminated by gases from the light produced by energy sources (Benea et al., 2014). Ni–TiO$_2$ nanocomposite coatings have been investigated by several researchers due to its superior anticorrosion performance, mechanical properties, and high photo electrochemical activity (Mohajeri et al., 2015). These coatings have been extensively used in many application fields, such as automotive parts, printed circuitry, electrical contacts, engine cylinders, high pressure valves, aerospace, medical devices, marine, nuclear field, and soft magnetic materials, for magnetic recording (Parida et al., 2011).

Ni matrix composites reinforced by TiO$_2$ nanoparticles can be successfully synthesized by electrodeposition utilizing either sulfamate or Watts plating baths (Spanou et al., 2009). During this process, the powder particles are suspended in a conventional electrolyte and are captured in the growing metal coating (Abdel Aal and Hassan, 2009).

Important process parameters for the production of electrodeposited composite coatings are current density, temperature, particle size, concentration, and bath composition. It is important to adjust the process parameters in order to control the properties of the produced composite coatings that depend on the amount of incorporated particles and their distribution in the metal matrix, as well as, on the microstructural characteristics of the metal matrix (Vaezi et al., 2008).

In the present work, Ni–TiO$_2$ nanocomposite coatings were produced on steel substrates by means of electrodeposition process. Effects of current density and TiO$_2$ nanoparticle size on the structure, mechanical, and corrosive properties of the coatings were investigated.

EXPERIMENTAL

First of all, TiO$_2$ nanoparticles were prepared by sol–gel technique. Titanium tetraisopropoxide was used as Ti precursor, glacial acetic acid as catalyst, and 2-propanol as solvent during the process. At the final step of the preparation of TiO$_2$ nanoparticles, they were heat-treated at 500°C for 1 h. Ni–TiO$_2$ nanocomposite coatings on steel substrates were electrodeposited from a standard nickel Watts bath (composition is given in **Table 1**) with 1 g l^{-1} concentration TiO$_2$ nanoparticles and different particle sizes (≈80 and 50 nm). All process parameters are given in **Table 2**. It is well-known that the dispersion of ceramic nanoparticles in

a plating bath is a very important stage of the electrodeposition process that strongly influences the nanocomposite properties. The Watts bath containing TiO$_2$ nanoparticles was stirred by means of a mechanical stirrer for 24 h before electrodeposition process. During electrodeposition, the electrolyte was magnetically stirred at the speed of about 200 rpm in order to keep the TiO$_2$ nanoparticles in suspension. Distance between the nickel anode and steel cathode was 7 cm. Pure Ni coatings were also deposited in order to make comparison with Ni–TiO$_2$ nanocomposite coatings. Nomenclature of pure Ni and Ni–TiO$_2$ nanocomposite coatings are given in **Table 3**.

The phase analysis of the deposited films was analyzed by X-ray diffractometer (XRD, Rigaku D/max-2200/PC) with grazing incident of 1° at 40 kV and 36 mA using CuKα radiation. The surface morphology and elemental composition of the obtained coatings were examined using a scanning electron microscope (SEM) equipped with an energy dispersive spectrometry (EDS) system (SEM/EDS, JEOL JSM 6060). Elemental mapping was also studied in order to illustrate the distribution of TiO$_2$ nanoparticles in Ni matrix.

Nanoindentation tests were carried out using a NanoTest instrument (Fischer-Cripps Lab. Pty. Ltd., Model B), using a Berkovich indenter with a face angle of 65.3°, which allows recording penetration depth as a function of applied loads with high load and displacement resolution. The surface roughness of coatings was measured by Ambios XP-2 Surface Profilometer. In order to minimize substrate effects, a maximum load of
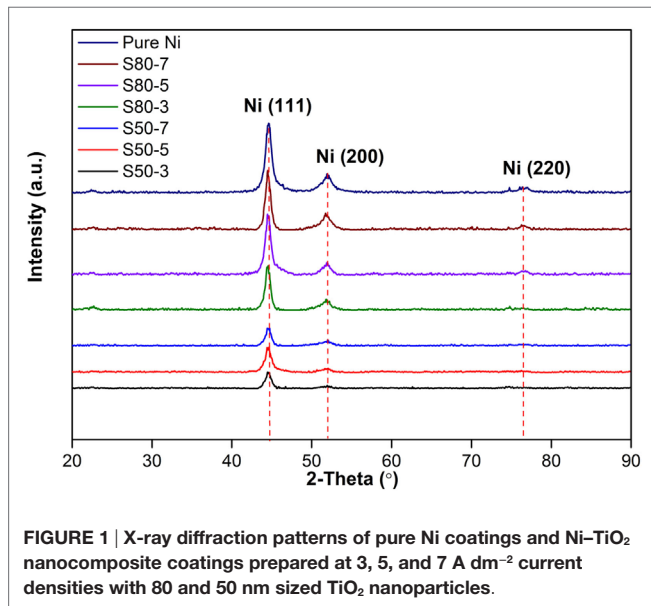
TABLE 1 | Composition of Watts bath.

Chemicals	Amount
NiSO$_4$·6H$_2$O	275 g l^{-1}
NiCl$_2$·6H$_2$O	50 g l^{-1}
H$_3$BO$_3$	40 g l^{-1}
Saccharin	10 ml l^{-1}
Sodium lauryl sulfate	0.5 ml l^{-1}

TABLE 2 | Electrodeposition parameters of Ni–TiO$_2$ nanocomposite coatings.

Electrodeposition parameters	
TiO$_2$ particle size	≈50 and ≈80 nm
Nanoparticle concentration	1 g l^{-1}
Coating duration	10 min
Current density	3, 5, and 7 A dm^{-2}
Bath temperature	45°C
Circulation rate of bath	200 rpm

TABLE 3 | Nomenclature of pure Ni and Ni–TiO$_2$ nanocomposite coatings.

Concentration of TiO$_2$	Size of TiO$_2$	Current density (A dm^{-2})		
		3	5	7
	–	Ni-3	Ni-5	Ni-7
1 g l^{-1} TiO$_2$	80 nm	S80-3	S80-5	S80-7
	50 nm	S50-3	S50-5	S50-7

FIGURE 1 | X-ray diffraction patterns of pure Ni coatings and Ni–TiO$_2$ nanocomposite coatings prepared at 3, 5, and 7 A dm^{-2} current densities with 80 and 50 nm sized TiO$_2$ nanoparticles.

150 mN was applied for measurements, which corresponds to a maximum penetration depth of ≈1000 nm. The holding time at the maximum load was of 5 s in order to minimize the creep effect, which may change the unload curve shape, affecting the final values of the coatings. The Elastic modulus (E) and Hardness (H) values were average of five measurements performed by applying the indenter on different areas of each investigated surface. Hardness (H) and elastic modulus (E) were calculated from the load–displacement curves according to the procedure outlined by Oliver and Pharr (Oliver and Pharr, 1992; Bull, 2005).

The corrosion measurements were carried out in 3.5 wt.% NaCl solution at room temperature using a Gamry potentiostat/galvanostat system controlled by the Gamry Framework software and Echem Analyst software, for the acquisition and analysis of electrochemical data. A conventional three-electrode cell was used for the corrosion experiments. Graphite electrode, Ag/AgCl, and prepared coatings were used as counter electrode, reference electrode, and working electrode, respectively. Measurement of the open circuit potentials (OCP) were performed in the test

FIGURE 2 | Surface morphologies of (A–C) pure Ni coatings, Ni–TiO$_2$ nanocomposite coatings prepared with 80 nm sized nanoparticles (D–F), and 50 nm sized nanoparticles (G–I) at 1 g l^{-1} concentration and 3, 5, and 7 A dm^{-2} current densities.
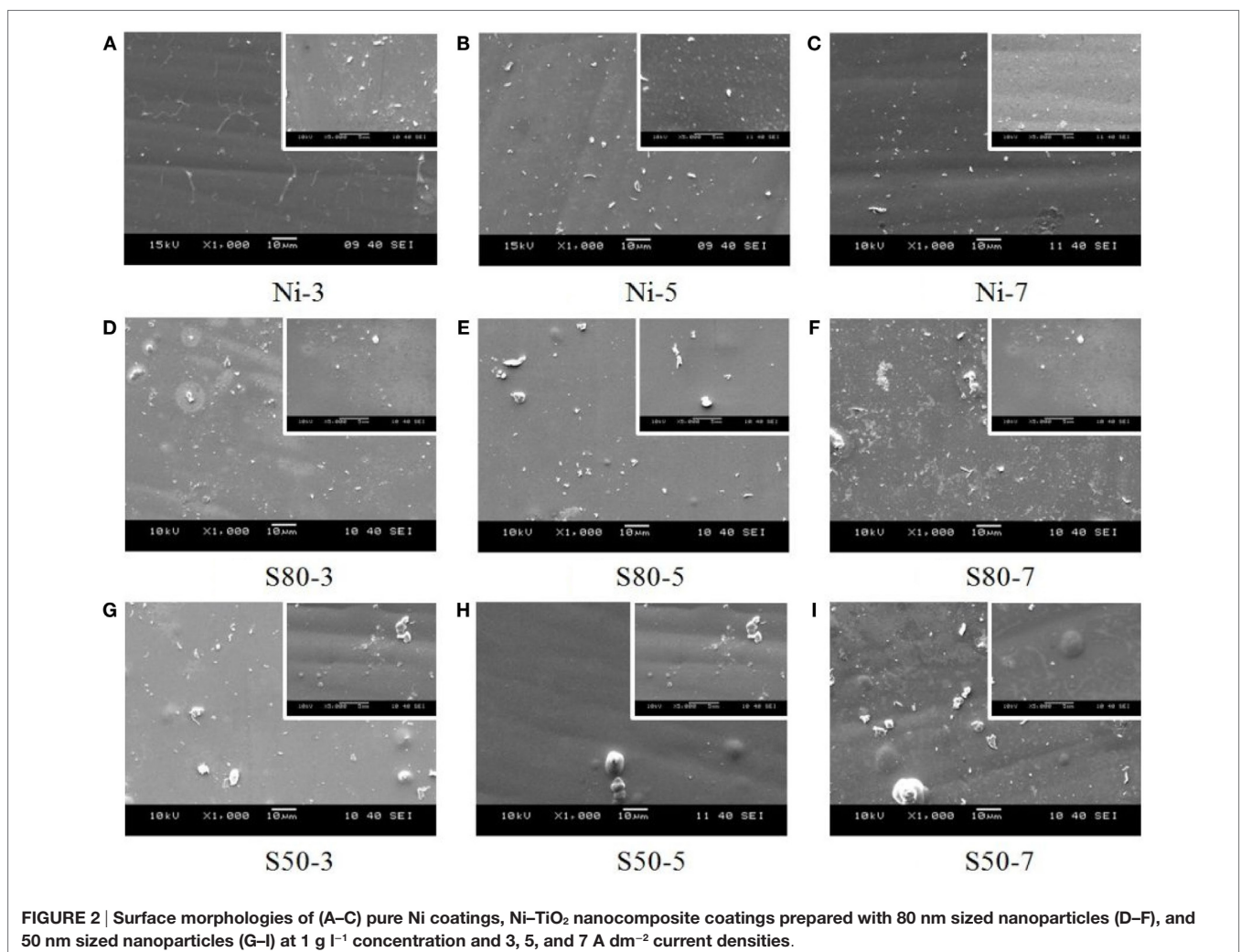
solution for 60 min. The potentiodynamic curves were obtained sweeping potential, starting at OCP, from −0.5 V vs. Ag/AgCl to 0.5 V vs. Ag/AgCl at a scan rate of 0.5 mV/s. Effect of UV illumination on the corrosion properties of nanocomposite coatings were also investigated using conventional three-electrode cell in order to investigate the possible application of Ni–TiO₂ nanocomposite coatings for the photocathodic protection. Measurement of the OCPs was performed under UV illumination by using Hamamatsu-L9588-01A light source and 250 W Hg-Xenon (Hamamatsu-L10852) lamp with wavelength of ≈365 nm as a source of irradiation. UV illumination was turned off afterward OCP potential measurement for 60 min, and then Tafel and potentiodynamic measurements were conducted at dark conditions.

RESULTS AND DISCUSSION

X-ray diffractometer patterns of coatings produced at different particle sizes of TiO₂ nanoparticles in the nickel electrolyte and different current densities are shown in **Figure 1**. All the deposited coatings are characterized by similar XRD patterns showing only Ni diffraction peaks. The XRD pattern is characterized by (111), (200), and (220) diffraction peaks of Ni phase (JCPDS 70-1849). The most intensive peak is located at $2\theta = 44.48°$ and corresponds to the Ni (111) reflection. It is obvious from the pattern that peak intensities increase with increasing current density from 3 to 7 A dm⁻² for both nanocomposite coatings produced at different particle sizes of TiO₂ nanoparticles. On the other hand, as is evident from XRD results, the addition of TiO₂ nanoparticles to Ni matrix and decrement of TiO₂ nanoparticles size from 80 to 50 nm results in a decrease of Ni phase peak intensities, and this may be interpreted as a contribution of nanoparticles to the coating structure causes such a change at the diffraction pattern. Daneshvar-Fatah and Nasirpouri (2014) have reported similar results in their study.

Figure 2 depicts the surface morphologies of pure Ni and Ni–TiO₂ nanocomposite coatings prepared at different current densities with different TiO₂ nanoparticles sizes. Higher magnification (5000×) of the SEM images was given at the top right-hand corner of each image for all samples. In general, all surface morphologies are crack-free and have homogeneous, smooth, and uniform surface distribution. EDS mapping results of Ni–TiO₂ nanocomposite coatings, prepared at 7 A dm⁻² current density, are illustrated in **Figure 3** as an example. Both the Ni composition and the TiO₂ nanoparticles distribution are homogeneous.

Nanoindentation is a suitable technique to measure mechanical properties of nanostructures (Wang et al., 2014). Representative load–displacement curves of the investigated coatings are displayed in **Figure 4**. The maximum indentation depth at 150 mN applied load (≈1000 nm) is less than 1% of the coating thickness and twice as much of surface roughness, excluding any influence of the substrate on the experimental results. The surface roughness has a significant influence on both hardness and elastic modulus of coatings determined from the nanoindentation tests. In order to rule out the influence of surface quality, the indentation depth should be much greater than the size of surface roughness (Jiang et al., 2008). The maximum penetration depth achieved at the end of the loading is smaller for the Ni–TiO₂ nanocomposite coating, suggesting that the TiO₂ nanoparticles play a reinforcing role, increasing the hardness of the nanocomposite coating. Elastic Modulus (E) and Hardness (H) of nanocomposite coatings are listed in **Table 4**. It was found that the both (E) and (H) values of Ni–TiO₂ nanocomposite coatings are higher than that of pure Ni coating prepared under the same conditions. According to Orowan's theory (Hosford, 2005), hard reinforcing particles force moving dislocations into bowing out between them, hindering their motion and leaving behind dislocation loops, which increase the stress required for the propagation of other incoming dislocations. This mechanism becomes more active
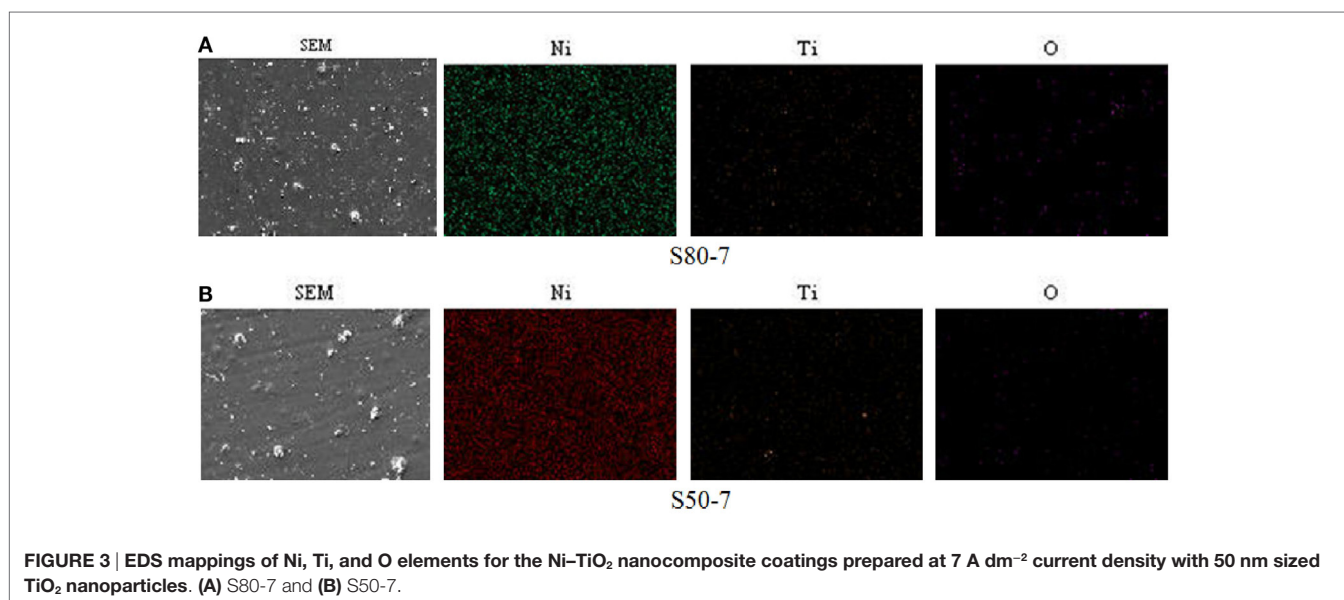

FIGURE 3 | EDS mappings of Ni, Ti, and O elements for the Ni–TiO₂ nanocomposite coatings prepared at 7 A dm⁻² current density with 50 nm sized TiO₂ nanoparticles. **(A)** S80-7 and **(B)** S50-7.
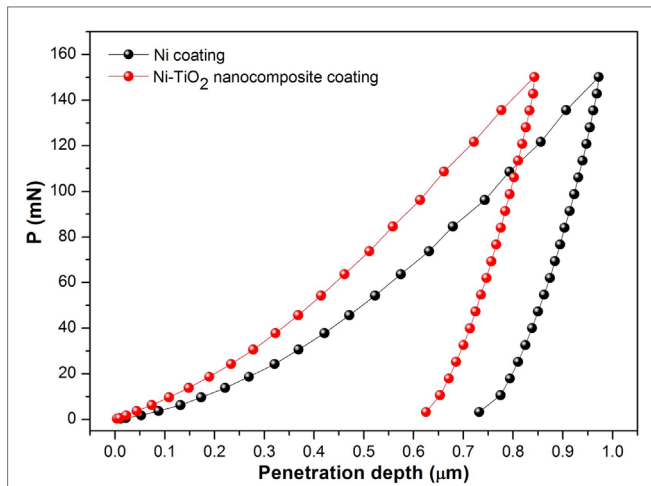
FIGURE 4 | Representative load–displacement nanoindentation curves corresponding to the Ni coating and Ni–TiO₂ nanocomposite coating.

TABLE 4 | Mechanical properties of nanocomposite coatings.

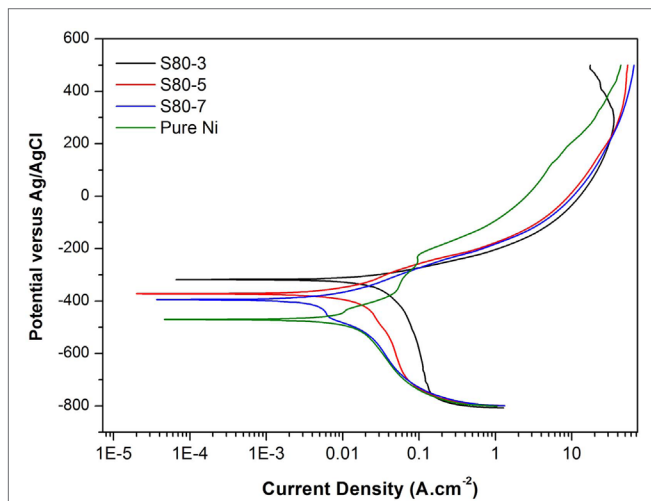| Coating	H (GPa)	E (GPa)	H/E	H^3/E^2
Ni-3	8.51	262.67	0.032	0.0089
S80-3	9.98	313.14	0.032	0.0101
S50-3	9.24	266.14	0.035	0.0111
Ni-5	9.71	250.12	0.039	0.0146
S80-5	11.88	300.73	0.040	0.0185
S50-5	11.60	280.06	0.041	0.0199
Ni-7	10.92	295.15	0.037	0.0149
S80-7	11.61	307.95	0.038	0.0165
S50-7	12.06	305.5	0.039	0.0188

FIGURE 5 | Potentiodynamic polarization curves of pure Ni and Ni–TiO₂ nanocomposite coatings deposited with 80 nm sized TiO₂ nanoparticles at 1 g l⁻¹ concentration and 3, 5, and 7 A dm⁻² current densities.

FIGURE 6 | Potentiodynamic polarization curves of pure Ni and Ni–TiO₂ nanocomposite coatings deposited with 50 nm sized TiO₂ nanoparticles at 1 g l⁻¹ concentration and 3, 5, and 7 A dm⁻² current densities.

TABLE 5 | Corrosion potential (E_{cor}) and corrosion current density (I_{cor}) values of pure Ni and Ni–TiO₂ nanocomposite coatings.

	E_{cor} (mV)	I_{cor} (A cm⁻²)
S80-3	−318	3.25×10^{-6}
S80-5	−371	1.36×10^{-6}
S80-7	−394	3.76×10^{-6}
S50-3	−277	0.83×10^{-6}
S50-5	−295	0.99×10^{-6}
S50-7	−326	1.47×10^{-6}
S80-3-UV	−240	1.79×10^{-7}
S80-5-UV	−342	0.90×10^{-6}
S80-7-UV	−336	1.29×10^{-6}
S50-3-UV	−249	3.47×10^{-7}
S50-5-UV	−326	1.03×10^{-6}
S50-7-UV	−309	1.02×10^{-6}
Pure Ni	−407	4.09×10^{-6}

with increasing volume fraction and smaller size of the particles (Miguel et al., 2015). In our case, the TiO₂ nanoparticles' low content and distribution ru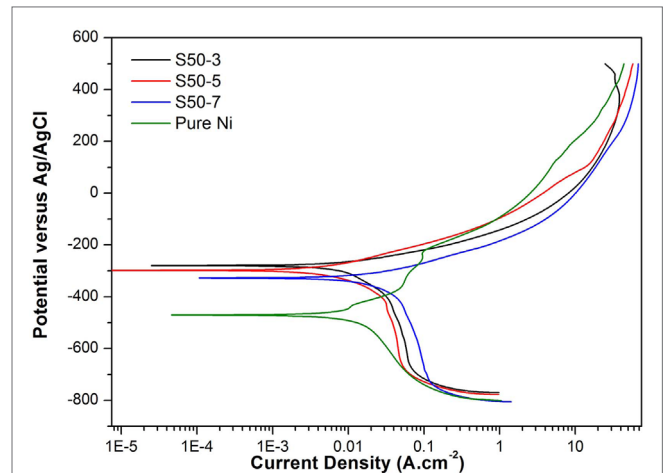led out the possibility of a significant role in the whole strengthening of the nanocomposite coatings. Additionally, it can be noticed that with increasing current density, there is a slight increase at E and H values of coatings. By an increase in current density, crystallite and grain size refinement occur, which results in increase in grain boundary fraction. Grain boundaries hinder dislocation motion, and this is one of the main causes of strengthening (Daneshvar-Fatah and Nasirpouri, 2014). Additionally, wear resistance is often correlated to mechanical parameters, such as H/E and H^3/E^2 ratios, which provide simultaneous information about resistance to plastic deformation and elastic properties of materials (Sakharova et al., 2010). Based on these parameters, the coating S50-5 is expected to exhibit higher tribological performance.

Potentiodynamic polarization curves of Ni–TiO₂ nanocomposite coatings are presented in **Figures 5** and **6**. Electrochemical parameters of the corrosion potential (E_{cor}) and corrosion current density (I_{cor}) were derived from Tafel extrapolation method, and the results are summarized in **Table 5**. E_{cor} value of Ni–TiO₂ nanocomposite coatings with 80 and 50 nm nanoparticles
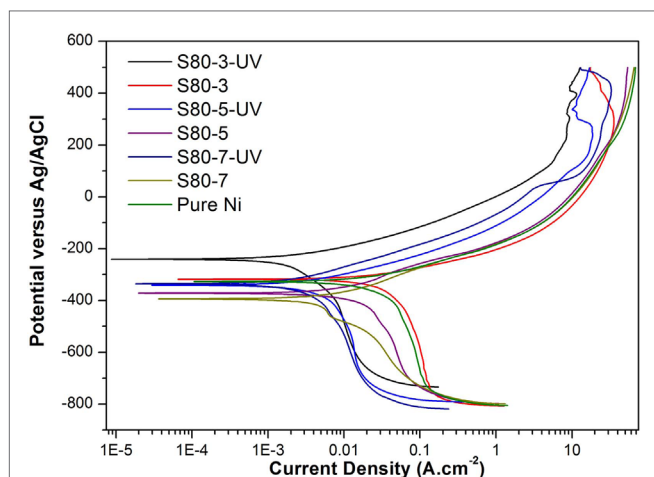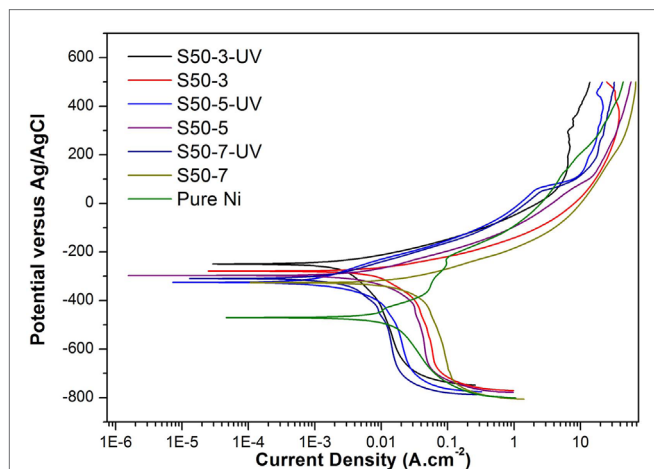
FIGURE 7 | Potentiodynamic polarization curves under the effect of UV illumination of pure Ni and Ni–TiO$_2$ nanocomposite coatings deposited with 80 nm sized TiO$_2$ nanoparticles at 1 g l^{-1} concentration and 3, 5, and 7 A dm^{-2} current densities.

FIGURE 8 | Potentiodynamic polarization curves under the effect of UV illumination of pure Ni and Ni–TiO$_2$ nanocomposite coatings deposited with 50 nm sized TiO$_2$ nanoparticles at 1 g l^{-1} concentration and 3, 5, and 7 A dm^{-2} current densities.

deposited at lower current densities shifted to noble direction. A higher corrosion resistance is commonly associated to a higher E_{OC} value. Obtained results show that corrosion resistance of nanocomposite coatings deposited at 3 A dm^{-2} current density are higher than the coatings prepared at higher current density

values. The electrochemical characteristics of nanocomposite coatings were also investigated under UV illumination, and the results are illustrated in **Figures 7** and **8**. UV illumination was applied during OCP measurement, and afterward it was turned off, and then Tafel and potentiodynamic measurements were conducted at dark conditions. Nanocomposite coatings illuminated with UV light exhibit better corrosion resistance compared to visible light measurements.

CONCLUSION

Ni matrix nanocomposite coatings have been produced by the electrodeposition process on steel substrates. The microstructure and mechanical properties of the films were studied, obtaining the following results:

– All the deposited coatings are characterized by similar XRD patterns showing only Ni diffraction peaks. Generally, peak intensity of the coatings increases with increasing current density values, and contribution of nanoparticles to the coating structure causes a decrease of Ni phase peak intensities.
– All surface morphologies are crack-free, homogeneous, and TiO$_2$ nanoparticles in the coating structure have uniform surface distribution.
– Both E and H values of Ni–TiO$_2$ nanocomposite coatings are higher than that of pure Ni coating prepared under the same conditions indicating better mechanical properties of nanocomposite coatings.
– Corrosion resistance of nanocomposite coatings deposited at 3 A dm^{-2} current density are higher than the coatings prepared at higher current density values and pure Ni coatings. Additionally, UV illumination during OCP measurements have an affirmative effect on corrosion resistance, especially for nanocomposite coating prepared with 50 nm sized TiO$_2$ nanoparticles.

AUTHOR CONTRIBUTIONS

IB and NA: manuscript preparation. MT and EC: literature review and introduction. TKD, SY, OB, and TD: experimental studies.

ACKNOWLEDGMENTS

REFERENCES

Abdel Aal, A., and Hassan, H. B. (2009). Electrodeposited nanocomposite coatings for fuel cell application. *J. Alloys Comp.* 477, 652–656. doi:10.1016/j.jallcom.2008.10.116

Beltowska-Lehman, E., Indyka, P., Bigos, A., Szczerba, M. J., and Kot, M. (2016). Effect of hydrodynamic conditions of electrodeposition process on microstructure and functional properties of Ni-W/ZrO2 nanocomposites. *J. Electroanal. Chem.* 775, 27–36. doi:10.1016/j.jelechem.2016.05.003

Benea, L., Danaila, E., and Celis, J. P. (2014). Influence of electro-codeposition parameters on nano-TiO$_2$ inclusion into nickel matrix and properties characterization of nanocomposite coatings obtained. *Mater. Sci. Eng. A* 10, 106–115. doi:10.1016/j.msea.2014.05.028

Bull, S. J. (2005). Nanoindentation of coatings. *J. Phys. D. Appl. Phys.* 38, R393–R413. doi:10.1088/0022-3727/38/24/R01

Daneshvar-Fatah, F., and Nasirpouri, F. (2014). A study on electrodeposition of Ni-noncovalnetly treated carbon nanotubes nanocomposite coatings with desirable mechanical and anti-corrosion properties. *Surf. Coat. Technol.* 248, 63–73. doi:10.1016/j.surfcoat.2014.03.023

Goldasteh, H., and Rastegari, S. (2014). The influence of pulse plating parameters on structure and properties of Ni-W-TiO2 nanocomposite coatings. *Surf. Coat. Technol.* 259, 393–400. doi:10.1016/j.surfcoat.2014.10.064

Gül, H., Kılıc, F., Uysal, M., Aslan, S., Alp, A., and Akbulut, H. (2012). Effect of particle concentration on the structure and tribological properties of sub-micron particle SiC reinforced Ni metal matrix composite (MMC) coatings produced by electrodeposition. *Appl. Surf. Sci.* 258, 4260–4267. doi:10.1016/j.apsusc.2011.12.069

Hosford, W. F. (2005). *Mechanical Behavior of Materials*. New York: Cambridge University Press.

Jiang, W. G., Su, J. J., and Feng, X. Q. (2008). Effect of surface roughness on nanoindentation test of thin films. *Eng. Fract. Mech.* 75, 4965. doi:10.1016/j.engfracmech.2008.06.016

Katamipour, A., Farzam, M., and Danaee, I. (2014). Effects of sonication on anticorrosive and mechanical properties of electrodeposited Ni-Zn-TiO2 nanocomposite coatings. *Surf. Coat. Technol.* 254, 358–363. doi:10.1016/j.surfcoat.2014.06.043

Lia, R., Hou, Y., and Liang, J. (2016). Electro-codeposition of Ni-SiO$_2$ nanocomposite coatings from deep eutectic solvent with improved corrosion resistance. *Appl. Surf. Sci.* 367, 449–458. doi:10.1016/j.apsusc.2016.01.241

Miguel, F. L., Müller, R., Mathur, S., and Mücklich, F. (2015). Microstructure and mechanical properties of electrodeposited Ni and Ni-matrix-nanocomposite thin films. *Mater. Sci. Eng. A* 646, 254–262. doi:10.1016/j.msea.2015.08.069

Mohajeri, S., Dolati, A., and Ghorbani, M. (2015). The influence of pulse plating parameters on the electrocodeposition of Ni-TiO$_2$ nanocomposite single layer and multilayer structures on copper substrates. *Surf. Coat. Technol.* 262, 173–183. doi:10.1016/j.surfcoat.2014.12.042

Oliver, W. C., and Pharr, G. M. (1992). An improved technique for determining hardness and elastic modulus using load and displacement sensing indentation experiments. *J. Mater. Res.* 7, 1564–1583. doi:10.1557/JMR.1992.1564

Parida, G., Chaira, D., Chopkar, M., and Basu, A. (2011). Synthesis and characterization of Ni-TiO2 composite coatings by electro-codeposition. *Surf. Coat. Technol.* 205, 4871–4879. doi:10.1016/j.surfcoat.2011.04.102

Sakharova, N. A., Fernandes, J. V., Oliveira, M. C., and Antunes, J. M. (2010). Influence of ductile interlayers on mechanical behavior of hard coatings under depth-sensing indentation: a numerical study on TiAlN. *J. Mater. Sci.* 45, 3812–3823. doi:10.1007/s10853-010-4436-1

Spanou, S., Pavlatou, E. A., and Spyrellis, N. (2009). Ni/nano-TiO$_2$ composite electrodeposits: textural and structural modifications. *Electrochim. Acta* 54, 2547–2555. doi:10.1016/j.electacta.2008.06.068

Thurber, C. R., Ahmad, Y. H., Sanders, S. F., Al-Shenawa, A., D'Souza, N., Mohamed Adel, M. A., et al. (2016). Electrodeposition of 70-30 CuNi nanocomposite coatings for enhanced mechanical and corrosion properties. *Curr. Appl. Phys.* 16, 387–396. doi:10.1016/j.cap.2015.12.022

Vaezi, M. R., Sadrnezhaad, S. K., and Nikzad, L. (2008). Electrodeposition of Ni-SiC nano-composite coatings and evaluation of wear and corrosion resistance and electroplating characteristics. *Colloids Surf. A Physicochem. Eng. Asp.* 315, 176–182. doi:10.1016/j.colsurfa.2007.07.027

Walsh, F. C., and Leon, P. (2014). A review of the electrodeposition of metal matrix composite coatings by inclusion of particles in a metal layer: an established and diversifying technology. *Trans. IMF* 92, 83–98. doi:10.1179/0020296713Z.000000000161

Wang, Y., Chen, W., Shakoor, A., Kahraman, R., Lu, W., Yan, B., et al. (2014). Ni-P-TiO$_2$ composite coatings on copper produced by sol-enhanced electroplating. *Int. J. Electrochem. Sci.* 9, 4384–4393.

Yang, X. Y., Li, K., Peng, X., and Wang, F. (2009). Beneficial effects of Co^{2+} on co-electrodeposited Ni-SiC nanocomposite coating. *Trans. Nonferrous Met. Soc. China* 19, 119–124. doi:10.1016/S1003-6326(08)60238-1